Modification of the Condensed 3-D TLM Node to Improve Modeling of Conductor Edges

J. S. Nielsen, *Member, IEEE,* and W. J. R. Hoefer, *Senior Member, IEEE*

***Abstract*—A modified condensed node TLM structure is proposed which, when used in conjunction with the conventional condensed node, improves the field simulation in the vicinity of conductive edges. This results in a substantial improvement in modeling accuracy of stripline and finline type structures.**

I. Introduction

THE condensed TLM node, initially developed by Johns [1], has superior dispersion characteristics than the expanded TLM and leap-frog FD–TD formulations for a given node density [2]. Hence, it should be possible to accurately model transmission line structures using the condensed node.

Unfortunately, significant errors occur when conductor edges, like those found in stripline structures, are modeled by Dirichlet boundary walls located halfway between nodes in the TLM mesh, as pointed out by Muller [3]. One example of these errors can be found in the TIM simulation of an axial strip in a rectangular waveguide performed by Eswarappa and Hoefer [4]. A sufficient node density was used such that dispersion effects were negligible. However, the resonant frequency of the strip, calculated with TLM, was 10% lower than predicted theoretically, which is unacceptable.

To explain the origin of these errors, consider the conductor edge modeled as a truncated Dirichlet boundary between node layers as illustrated in Fig. 1. Nodes 5 and 6, immediately adjacent to the conductor edge, share a corner that coincides with the conductor edge and should therefore couple strongly with the resultant edge current. However, in the condensed node formulation, the coupling is only indirect through the nodes 3 and 4 that represents a weaker and delayed interaction. Hence, the errors can be attributed to an insufficient coupling of the simulated strip edge current with the surrounding fields.

Increased interaction is possible by connecting nodes 5 and 6, in Fig. 1, directly to the conductor edge via shorting stubs. This has been demonstrated, in the 2-D shunt node mesh, to significantly improve simulation results [5]. For the 3-D condensed node mesh, we are proposing another approach which involves modifying the condensed node such that the conductor strip is embedded into the node to achieve higher coupling. This results in two new node structures that are illustrated in Fig. 2 as the "half node" and the "edge node".

Manuscript received October 9, 1991.

J. S. Nielsen is with Lockheed Canada Inc., 1 Iber Road, Stittsville, ON K2S 1E6, Canada.

W. J. R. Hoefer is with the Department of Electrical Engineering, University of Ottawa, ON K1N 6N5, Canada.

IEEE Log Number 9106528.

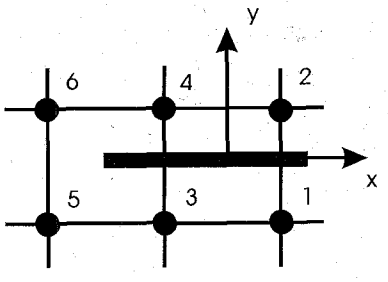

Fig. 1. Conventional modeling of a conductor strip.

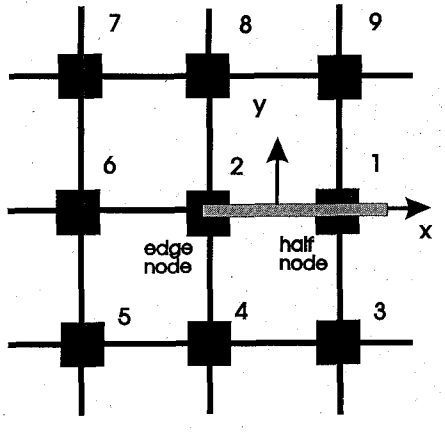

Fig. 2. Half node modeling of conductor strip.

The scattering matrix for the half node and edge node are discussed in Sections II and III. A demonstration of the improved accuracy possible by using these new node types is given in Section IV using a simple stripline resonator test model.

II. Scattering Matrix Of The Half Node

The half node is modeled after the condensed node and therefore, retains the energy and current conservation properties, as well as the dispersion characteristics. A half node configuration for the case when the conductor is in the *x-z* plane is shown in Fig. 3. The conductor sheet splits ports 2, 3, 7, and 10 into eight ports 2a, 3a, 7a, 10a above the conductor and 2b, 3b, 7b, 10b below the conductor. The impedance of these split ports is half the impedance of the regular ports. Electric fields tangential to the conductor surface are zero. Hence, ports 1, 8, 5, and 9 are omitted. An infinite conductor sheet was asssumed when determining the port scattering parameters of the half node.

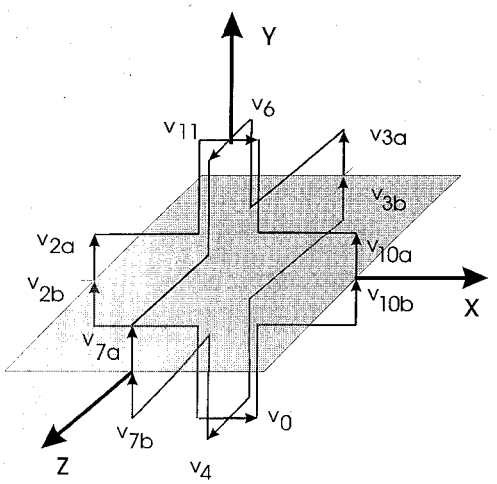

Fig. 3. Half node configuration.

The reflected and incident voltage vectors are defined as

$$\boldsymbol{V^r} = \begin{pmatrix} V_0^r \\ V_{2a}^r \\ V_{2b}^r \\ V_{3a}^r \\ V_{3b}^r \\ V_4^r \\ V_6^r \\ V_{7a}^r \\ V_{7b}^r \\ V_{10a}^r \\ V_{10b}^r \\ V_{11}^r \end{pmatrix} \qquad \boldsymbol{V^i} = \begin{pmatrix} V_0^i \\ V_{2a}^i \\ V_{2b}^i \\ V_{3a}^i \\ V_{3b}^i \\ V_4^i \\ V_6^i \\ V_{7a}^i \\ V_{7b}^i \\ V_{10a}^i \\ V_{10b}^i \\ V_{11}^i \end{pmatrix}, \tag{1}$$

which are related as $V^r = SV^i$ where the scattering matrix, S, is given by

$$S = \frac{1}{2}\begin{pmatrix} 0 & 0 & 2 & 0 & 0 & 0 & 0 & 0 & 0 & 0 & -2 & 0 \\ 0 & 0 & 0 & 1 & 0 & 0 & 0 & 1 & 0 & 0 & 0 & -1 \\ 1 & 0 & 0 & 0 & 1 & 0 & 0 & 0 & 1 & 0 & 0 & 0 \\ 0 & 1 & 0 & 0 & 0 & 0 & -1 & 0 & 0 & 1 & 0 & 0 \\ 0 & 0 & 1 & 0 & 0 & 1 & 0 & 0 & 0 & 0 & 1 & 0 \\ 0 & 0 & 0 & 0 & 2 & 0 & 0 & 0 & -2 & 0 & 0 & 0 \\ 0 & 0 & 0 & -2 & 0 & 0 & 0 & 2 & 0 & 0 & 0 & 0 \\ 0 & 1 & 0 & 0 & 0 & 0 & 1 & 0 & 0 & 1 & 0 & 0 \\ 0 & 0 & 1 & 0 & 0 & -1 & 0 & 0 & 0 & 0 & 1 & 0 \\ 0 & 0 & 0 & 1 & 0 & 0 & 0 & 1 & 0 & 0 & 0 & 1 \\ -1 & 0 & 0 & 0 & 1 & 0 & 0 & 0 & 1 & 0 & 0 & 0 \\ 0 & -2 & 0 & 0 & 0 & 0 & 0 & 0 & 0 & 2 & 0 & 0 \end{pmatrix}. \tag{2}$$

III. Scattering Matrix Of The Edge Node

The edge node for the left strip edge, illustrated in Fig. 2, is essentially the same as the half node except for the ports that connect to node 6. To explain the differences, consider first the half node of Fig. 3. At each time interval a pair of voltages V_{2a}^r and V_{2b}^r are generated that must be coupled into port 10 of the adjacent conventional condensed node. The symmetrical component, $\frac{1}{2}(v_{2a}^r + V_{2b}^r)$ couples directly into port 10 of the adjacent node such that

$$V_{10}^i = V_{2a}^r + V_{2b}^r.$$

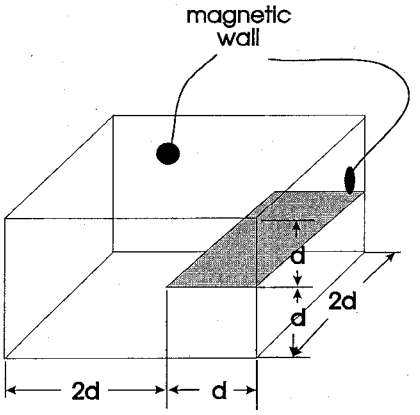

Fig. 4. Half wavelength stripline resonator test circuit.

The antisymmetric component, $\frac{1}{2}(V_{2b}^r - V_{2a}^r)$, is reflected back into ports 2a and 2b with a reflection coefficient of unity. The reason for this is that the antisymmetric voltage is directly proportional to the current flowing on the conductor strip which must be zero at the conductor edge. Hence,

$$V_{2a}^i = \frac{1}{2}(V_{2a}^r - V_{2b}^r)$$
$$V_{2b}^i = \frac{1}{2}(V_{2b}^r - V_{2a}^r).$$

V_{2a}^i and V_{2b}^i can be inserted into the node during the next update interval, however, this would inadvertently result in a capacitive stub connected to the antisymmetric voltage of port 2. This extraneous capacitive stub is not correct and must be removed by scattering the incident antisymmetric voltage during the present update cycle. In summary, the resulting reflected port voltages are determined by using the scattering matrix for the half node with the scattered contribution from the antisymmetric voltage incident at port 2a and 2b superimposed.

IV. Discussion And Results

A half-wavelength stripline resonator, shown in Fig. 4, was selected to demonstrate the improved accuracy obtained by using the half and edge nodes to simulate the strip. The

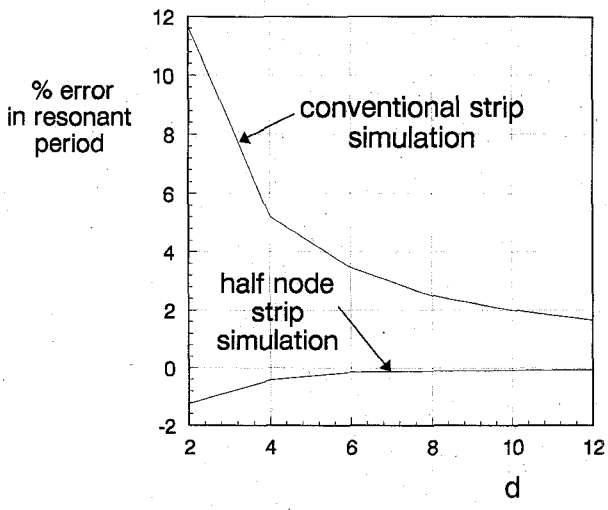

Fig. 5. Relative error in resonant period of stripline resonator.

dimensions in Fig. 4 are given in terms of the number of nodes used. The relative error in the resonant frequency as a function of the parameter "d" in Fig. 4 is given in Fig. 5. The results are compared with the conventional method of simulating the strip as a Dirichlet boundary between nodes as illustrated in Fig. 1. There is a substantial improvement in accuracy possible by incorporating the half node into the TLM mesh.

Another important feature is that Dirichlet boundaries can now be positioned either halfway between nodes or through the nodes, which increases the geometric modeling accuracy.

REFERENCES

[1] P. B. Johns, "A symmetrical condensed node for the TLM method," *IEEE Trans. Microwave Theory Tech.*, vol. MTT-35, no. 4, pp. 370–377, Apr. 1987.

[2] J. Nielsen and W. Hoefer, "A complete dispersion analysis of the condensed node TIM mesh," *IEEE Trans. Magn.*, vol. 27, pp. 3982–3985, Sept. 1991.

[3] U. Huller, "Analyse plananer Wellenleiter und Diskontinuitaten im zeitbereich mit TLM-Methode," undergraduate thesis, UniversitatGesamthochschule_Duisburg, Jan. 1991

[4] Eswarappa and W. J. R. Hoefer, "Diakoptics and wideband dispersive absorbing boundaries in the 3-D TLM method with symmetrical condensed nodes," *IEICE Trans.* vol. E 74, no. 5, pp. 1242–50, May 1991.

[5] W. Hoefer, "CAD oriented modeling of electromagnetic fields in the time domain using TIM techniques," *IEEE Workshop on CAD Oriented Numerical Techniques for the Analysis of Microwave and MM-Wave Transmission Line Discontinuities and Junctions,* Stuttgard, Sept. 13, 1991, pp. 57–69.